Terrestrial Gamma-ray Flashes Can Be Detected with Radio Measurements of Energetic In-cloud Pulses during Thunderstorms

Fanchao Lyu[1,2], Steven A. Cummer[3*], Michael Briggs[4], David M. Smith[5], Bagrat Mailyan[6], Stephen Lesage[4]

[1]Nanjing Joint Institute for Atmospheric Sciences, Nanjing, Jiangsu, China

[2]State Key Laboratory of Severe Weather, Chinese Academy of Meteorological Sciences, Beijing, China

[3]Electrical and Computer Engineering Department, Duke University, Durham, North Carolina, USA

[4]CSPAR, University of Alabama in Huntsville, Huntsville, Alabama, USA

[5]Physics Department, University of California Santa Cruz, Santa Cruz, California, United States

[6]Center for Astro, Particle and Planetary Physics, New York University Abu Dhabi, Saadiyat Marina District, Abu Dhabi, UAE

* Correspondence to: cummer@ee.duke.edu

Key point:

- Positive polarity energetic in-cloud pulses produce TGFs with high-to-certain probability (74% - 100%)
- New TGFs previously missed by space-based detectors were found by ground detection of +EIPs
- Demonstrated that a subset of TGFs can be found from remote ground-based radio detection alone

Abstract

Many of the details of how terrestrial gamma-ray flashes (TGFs) are produced, including their association with upward-propagating in-cloud lightning leader channels, remain poorly understood. Measurements of the low-frequency radio emissions associated with TGF production continuously provide unique views and key insights into the electrodynamics of this process. Here we report further details on the connection between energetic in-cloud pulses (EIPs) and TGFs. With coordinated measurements from both the ground-based radio sensors and space-based gamma-ray detectors on the Fermi and RHESSI spacecraft, we find that all ten +EIPs that occurred within the searched space-and-time window are associated with simultaneous TGFs, including two new TGFs that were not previously identified by the gamma-ray measurements alone. The results in this study not only solidify the tight connection between +EIPs and TGFs, but also demonstrate the practicability of detecting a subpopulation of TGFs with ground-based radio sensors alone.

1. Introduction

Terrestrial gamma-ray flashes (TGFs) are a kind of high energy emissions (up to several tens of MeV) that are generated during thunderstorms and are generally detected by space-based gamma-ray photon detectors (*Fishman et al.,* 1994; *Smith et al.,* 2005; *Briggs et al.,* 2010; *Marisaldi et al.,* 2010; *Neubert et al.,* 2020). Ground-based radio measurements and modeling of the discharge processes associated with TGFs suggest that low frequency (LF) radio emissions are usually generated during TGF production (*Connaughton et al.,* 2010; *Cummer et al.,* 2011; *Lu et al.,* 2011; *Dwyer et al.,* 2012; *Dwyer & Cummer,* 2013; *Cummer et al.,* 2014; *Dwyer et al.,* 2017; *Lyu et al.,* 2018; *Roberts et al.,* 2018; *Pu et al.,* 2019; *Zhang et al.,* 2020), but the details of these LF signals still need further investigation.

More specifically, a recent study reported a distinct lightning process called energetic in-cloud pulses (EIPs) that occur during the propagation of some negative leaders and produce high equivalent peak current pulses (*Lyu et al.,* 2015; *Lyu & Cummer,* 2018). The similarity of the radio emissions between that associated with a subset of TGFs (*Lu et al.,* 2011; *Cummer et al.,* 2014) and that of EIPs raised the question of whether EIPs and TGFs two faces of the same phenomenon. Lyu et al. (*Lyu et al.,* 2016) addressed that question using 3 EIPs that were identified from radio measurements alone that occurred within the gamma-ray detection range (500 km horizontally) of the Fermi Gamma-ray Burst Monitor (GBM) instrument (*Briggs et al.,* 2010). The known location and time of these 3 EIPs enabled a search for associated TGF gamma-rays in a narrow 100-microsecond time window. Interestingly, all three events contained significant gamma-ray flux simultaneous with the EIPs, showing that the three EIPs were all also TGFs (*Lyu et al.,* 2016). In addition, the similar occurrence contexts (*Stanley et al.,* 2006; *Lu et al.,* 2010; *Shao et al.,* 2010; *Cummer et al.,* 2011;

71 *Østgaard et al.*, 2013; *Lyu et al.*, 2018; *Pu et al.*, 2019) and event occurrence frequency
72 between EIPs and TGFs within the Fermi-observed area further support the idea that at
73 least a significant fraction of EIPs are also TGFs (*Lyu et al.*, 2016). A recent study
74 from the observations with the Atmosphere Space Interactions Monitor (ASIM)
75 (*Neubert et al.*, 2019), onboard the International Space Station (ISS), showed a
76 terrestrial gamma-ray flash (TGF) associated with elves produced during the initial
77 leader of a lightning flash (*Neubert et al.*, 2020). The associated radio signal was likely
78 an EIP of positive polarity, which also confirmed the model study on the possible
79 relationship between TGFs and Elves through a common association with EIPs (*Liu et*
80 *al.*, 2017).

81 These studies suggested a strong connection between EIPs, TGFs, and other
82 phenomena. Even though only a subset (~10%) of TGFs are associated with the
83 extremely high equivalent peak current radio emissions of EIPs (*Lu et al.*, 2011;
84 *Cummer et al.*, 2014), this finding on the EIP-TGF relationship opens the possibility
85 that a portion of the overall TGF population could be identified from ground-based
86 radio measurements alone. The 3 out of 3 EIP-TGF pairs and their similar occurrence
87 contexts enabled the hypothesis that every +EIP is also a TGF (*Lyu et al.*, 2016). This
88 study aims for improved statistics to answer the two fundamental questions: Are all
89 EIPs identified from radio emissions alone also TGFs? And is it possible to detect a
90 subset of TGFs by searching the ground measurements of EIPs alone?

91 We report here the analysis of an enlarged, 5-year database of EIPs that occurred
92 during Fermi and RHESSI satellite overpasses. We find that a total of 10 out of 10
93 +EIPs are associated with detected TGFs that are essentially simultaneous with the EIPs.
94 This includes the 3 +EIPs previously reported by Lyu et al. (*Lyu et al.*, 2016), 5 new
95 EIPs associated with previously identified TGFs, and importantly 2 new EIP-TGFs that

were not previously identified from gamma-ray measurements alone. One of these was detected by the Fermi Gamma-ray Burst Monitor (GBM) (*Briggs et al.*, 2010), and one was detected by the Reuven Ramaty High Energy Solar Spectroscopic Imager (RHESSI) (*Smith et al.*, 2005). That 10 out of 10 independently identified +EIPs are also found to be simultaneous TGFs implies a high-to certain probability of 74%-100% that any given +EIP is also TGF. It is especially noteworthy that a search for +EIPs from the ground radio measurements alone identified two previously unreported TGFs from two different space-based platforms. This not only provides strong evidence of the connection between +EIPs and TGFs, but also demonstrates the practicability of detecting a subpopulation of TGFs from ground-based radio measurements alone.

2. Instrumentation

The analysis in this study was conducted with a comprehensive investigation of radio signals of +EIPs and the gamma-ray photons in a short time window of several hundred microseconds around the time of the +EIPs. +EIPs were identified from a combination of high peak current NLDN events and the corresponding radio emissions, which includes the low frequency (LF), very low frequency (VLF), and ultra-low frequency (ULF) radio sensors operated by Duke University (*Lyu et al.*, 2015; *Lyu et al.*, 2016). The +EIPs were identified with the same approach used by Lyu et al. (2016) by accumulating NLDN-reported lightning events above a peak current threshold (150 kA or 200 kA, depending on the year) and within a given maximum range (1000 or 2000 km, again depending on the year) from one of our LF radio sensors deployed around the United States. All the NLDN-reported positive ICs, positive CGs, and negative ICs that exceeded the peak current threshold were selected for waveform

120 analysis. We then used VLF and LF radio waveforms to classify each of these lightning
121 events as CG, NBE, or EIP based on the automated process described previously (*Lyu*
122 *et al.*, 2015). The positive EIPs were sorted out based on their radio signal polarity.

123 The +EIPs identified during two periods were analyzed in this study: either from
124 a four-year database between 2014 and 2017, or from the year 2012. The two periods
125 of +EIPs were selected corresponding to the two different space-based gamma-ray
126 detection platforms, respectively, which are the Fermi-GBM (*Briggs et al.*, 2010) and
127 the RHESSI gamma-ray detector (*Smith et al.*, 2005). This population of +EIPs is then
128 analyzed based on the horizontal distance from the Fermi or RHESSI satellite footprint
129 at the time, and for those events sufficiently close, we examine the gamma-ray counts
130 from each instrument at the precise time predicted by the known +EIP location and time.

131

132 **3. +EIPs identified during a four-year survey and the TGF signature of +EIPs**
133 **recognized by Fermi-GBM**

134 From the radio measurement database during 2014–2017, a total of 1334 events
135 were identified by the radio signals to be +EIPs. It included 69 events in two months
136 of 2014 and 403 events in 2015 that were reported by Lyu et al. (2016), and also
137 includes 450 events in 2016 and 412 events in 2017. Fermi operates as a nearly circular
138 orbit at the altitude of 565 km with an inclination of 25.6° and can effectively detect
139 the gamma-ray emissions within the horizontal range of about 600 km from its nadir
140 (*Briggs et al.*, 2010). With the location of +EIPs reported by NLDN and the position
141 of Fermi footprints, the horizontal distances between +EIPs and Fermi nadirs can be
142 obtained. Figure 1a shows the distribution of the horizontal distance between the +EIP
143 location (from NLDN) and the corresponding Fermi nadir point, and Figure 1b shows

the geographic distribution of the +EIPs.

As illustrated in Figure 1a, a total of 10 +EIPs were found to be located within 600 km away from the Fermi nadir at the +EIP time. The source time of each +EIP was obtained by subtracting the propagation time between the LF sensor and the +EIP source, which was supposed at the NLDN horizontal location and an altitude of 12 km (*Cummer et al.*, 2014; *Lyu et al.*, 2015; *Lyu et al.*, 2018; *Pu et al.*, 2019). Then an independent search of the gamma-ray photon times recorded by Fermi-GBM time-tagged events (TTE) data mode and detected by two bismuth germanate (BGO) scintillation detectors at the source time of each +EIP was conducted. For one of these +EIPs, the BGO count data are unavailable and this event is excluded from further analysis. For the remaining 9 +EIPs, the binned histograms of gamma-ray count times relative to the +EIP time are shown in Figure 1(c).

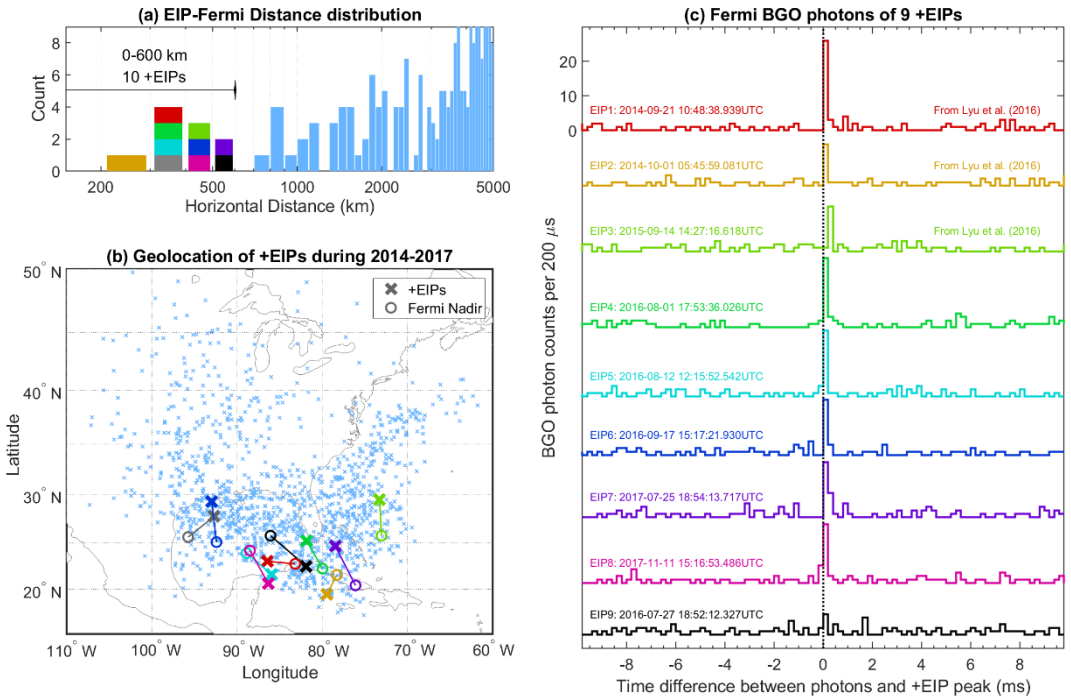

Figure 1. All +EIPs identified during 2014–2017 and gamma-ray photons of 9 +EIPs that also reported by Fermi as TGFs. (a) The distribution of the horizontal distance

between the NLDN location of each +EIP and the nadir of Fermi at +EIP time. Note that all the +EIPs were in the range of 263 km to ~20,000 km, but only those within the range of 5000 km of a Fermi nadir were illustrated in (a). The horizontal short line enclosed the +EIPs located less than 600 km from Fermi. (b) The geolocation of all the 1334 +EIPs (marked by the light blue crosses). The colorful crosses and the circles illustrated the location of the 10 +EIPs enclosed by the short line in (a) and the corresponding Fermi nadir positions. The small light blue crosses mark the geolocation of all other +EIPs with larger distances. (c) The source time difference between Fermi BGO photon counts (binned with 200 μs window) and the peak of the initial LF pulse of each +EIP.

3.1 EIP1 to EIP8 previously reported by Fermi-GBM as TGFs

The relative distance between the +EIP location and the Fermi nadir can be found in Figure 1(a) by the plots of different colors shown in Figure 1(c). As can be seen in Figure 1(c), EIPs 1–8 were associated with clear bursts of gamma-ray photons within a short time window around the expected time. These 8 TGFs were also identified by the Fermi general TGF identification criteria and reported to be TGFs (*Briggs et al.*, 2013). Three of these 8 of are those 3 already analyzed by Lyu et al. (2016) in a preliminary investigation on the relationship between +EIP and TGFs. Thus we show here that during the year 2016-2017, an additional 5 EIP-TGF pairs (EIP4 to EIP8) were found. Even though these 8 TGFs were previously identified, it should be emphasized that here they were found through a search that only used the radio waveforms, radio timing, and source location of the lightning.

As shown by the binned histogram plot in Figure 1(c), the peak time of the BGO gamma-ray count pulses and initial peak times for EIP4-EIP8 are aligned very well in the 200-μs bin window. These 8 events further show the very close association between +EIPs and TGFs in a short time window (usually ~200 μs).

3.2 EIP9 identifies a new Fermi TGF

EIP9 was located at 560 km from its corresponding Fermi nadir, with the relative distance and locations illustrated by the black plots in Figure 1(a) and 1(b). The histogram of original gamma-ray photons from both two BGO channels is shown by the black curve at the bottom of Figure 1(c). A weak pulse of gamma-ray photons during the short window of EIP9 can be seen, and this event was not reported as a TGF in the Fermi GBM database. However, a detailed investigation into the Fermi-GBM gamma-ray photon data indicates that EIP9 is in fact a weak TGF.

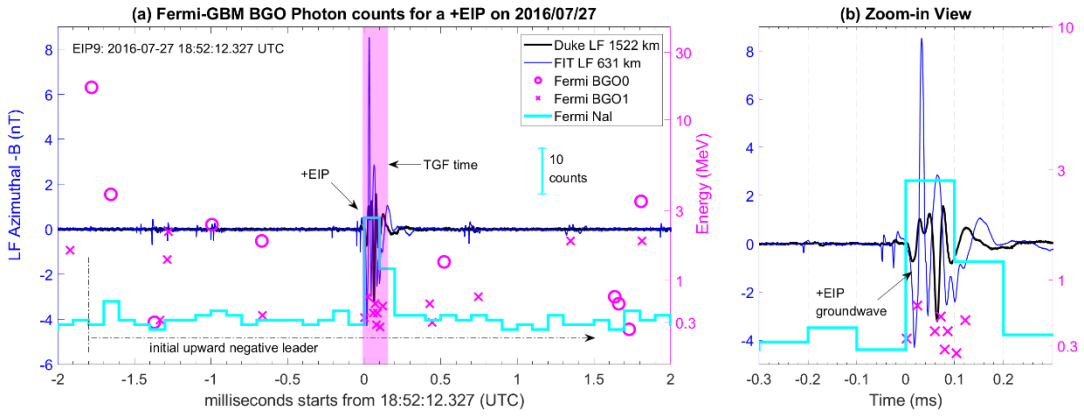

Figure 2. The radio signals (blue and black curves) of the EIP-producing leader and the Fermi-GBM detected BGO photon counts (magenta circles and crosses) and the NaI histogram (cyan stair plot) during the occurrence of EIP9 on Jul 27, 2016, at 18:52:12.327 (UTC).

Figure 2 shows the time association of the LF radio signal of EIP9 from two LF sensors (Duke and FIT) and the Fermi-GBM detected gamma-ray photons. Both times were shifted back to the source location of EIP9 by subtracting the speed-of-light propagation delays. The clear LF pulses both before and after EIP9 suggests that it was likely produced during an initial upward IC negative polarity leader approximately 1.8 ms after the leader initiation, which is a typical occurrence context of +EIPs (*Lyu et al.*, 2015). The magenta crosses and circles indicated the times of gamma-ray photons detected by two BGO detectors (BOG0 and BGO1), respectively. Note that there were no photons detected by BGO0 during the 1 ms window around EIP9, and BGO0 recorded only random background counts. Nevertheless, a burst of 8 BGO photons with energy of hundreds of keV from BGO1 and a histogram peak of 24 photons from sodium iodide (NaI) scintillation detectors (energy range of 8 keV to 1 MeV) (*Briggs et al.*, 2013) was aligned very well with EIP9 in a ~100 μs window. This strongly indicates that there was a TGF associated with EIP9. The magenta shadow in Figure 2(a) indicates the window when the TGF was produced, which is well consistent with the circumstance of EIP1–EIP8 shown in Figure 1(c).

TGFs are identified from the Fermi-GBM database using offline analysis of the TTE photon data (*Briggs et al.*, 2013). To reduce the number of false identification due to statistical fluctuations and to ensure sufficient signal to be able to reject cosmic rays effectively, the off-line search requires at least four counts in each BGO detector within a variable time window (*Briggs et al.*, 2013). However, this detection criterion introduces a dependence on the relative position between the spacecraft coordinates and the TGF source. Under certain viewing geometries, only one of the BGO detectors is expected to receive gamma-ray counts from a TGF due to shadowing by the spacecraft.

This limits the detection efficiency of some TGFs due to an unfavorable arrival direction in the spacecraft frame (*Roberts et al.,* 2018). And the low energy range of the BGO photons associated with EIP9 (ranging from 140 to 660 keV) is well consistent with the large offset from the Fermi nadir (560 km for EIP9) and that Fermi is outside of the main beam and observing Compton scattered photons, which dynamically decreases the energy of photons (*Østgaard et al.,* 2008; *Celestin & Pasko,* 2012; *Briggs et al.,* 2013; *Xu et al.,* 2019). This appears to be the reason that the TGF associated with EIP9 was not identified in the Fermi analysis. However, the data indicate that this is indeed a new TGF, and it was found through this search based on the ground-based measurement of radio signal and timing analysis.

4. A new RHESSI TGF identified by ground measurement of +EIPs

The gamma-ray counts detected by RHESSI were also examined to identify any TGF signatures of +EIPs. RHESSI was a NASA Small Explorer spacecraft designed to study x-rays and gamma rays from solar flares, with an orbit of inclination 38º and of altitude 600 km (*Smith et al.,* 2005). It covered most of Earth's thunderstorm zones and detected TGFs with geomagnetic latitudes up to ~50º and detected TGFs effectively for those occurred within 500 km horizontal range of the nadir point. Accounting for the availability of both the radio and photon data, +EIPs in the year 2012 were investigated. Although we archived only limited LF data during 2012, +EIPs were successfully identified from the VLF/ULF radio signals, which also showed distinguishable signatures of the EIP process. The search process was basically the same as that described by Lyu et al. (*Lyu et al.,* 2015).

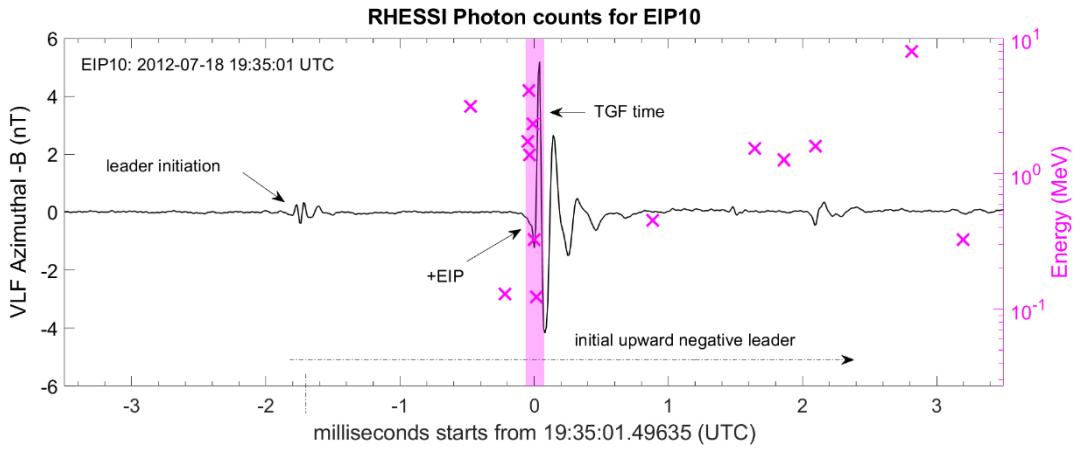

Figure 3. (a) The VLF radio waveform of the EIP-producing leader and the RHESSI detected photons during the occurrence of EIP10 on Jul 18, 2012, at 19:35:01 UTC. The burst of the photons and their energy were marked by the magenta crosses, with the magenta bar illustrates the time of a TGF.

For this portion of the analysis, we only focused on the NLDN-identified IC events with peak current above 100 kA and those located within 1000 km of the RHESSI footprint. During the calendar year of 2012, a total of 72 NLDN-reported high peak-current IC events fell into our initial data set. Then with careful investigation and event discrimination, a total of 13 +EIP events were identified from the archived VLF and ULF data. There is only one of these +EIPs (EIP10, hereinafter) that was located within 500 km (315 km) from the RHESSI nadir, which is the effective detection range of RHESSI. No TGF was reported in the RHESSI TGF catalog during the time window around EIP10.

However, the RHESSI gamma-ray photon data during a short window centered at the source time of EIP10 reveal that there was a TGF at this time. The radio signals measured by the Duke VLF sensor and photons detected by the RHESSI gamma-ray

detector during a 7-ms window were shown in Figure 3, with the times of both the radio signals and photons were shifted back to the source position of EIP10, which was assumed to be at 12 km above its NLDN ground location. EIP10 was reported by NLDN with a peak current of 195 kA. From the VLF signals recorded at 1279 km, a weak initiation pulse was identified at ~1.9 ms preceding EIP10. The radio pulses both before and after the main EIP pulse suggests an active lightning leader process during the EIP occurrence (*Lyu et al.*, 2015). It is remarkable to note that a burst of six photons with energy ranging from ~100 keV to 4.1 MeV were lined up in a 60-μs window of the initial VLF peak of EIP10. This agrees well with the scenario of EIP-associated Fermi TGFs shown in Figure 1(c) and Figure 2. Comparing to the random photons both before and after EIP10, the burst of high energy photons in such a short window strongly indicates a TGF associated with EIP10. This radio-based search process has thus identified 2 new TGFs, adding to the evidence that most and perhaps all +EIPs are also TGFs.

5. Analysis and Significance of EIP-TGF Relationship

Our search for +EIPs from radio and NLDN data required that either Fermi or RHESSI was sufficiently close to the source to detect any possible TGF but was otherwise unbiased from the perspective of TGFs. Of the 10 +EIPs that were sufficiently close to the satellites and for which gamma-ray count data are available, we have found that all 10 are associated with clear and unambiguous TGFs. It should be emphasized that while a +EIP implies a TGF with high certainty, this does not mean that a TGF implies a +EIP with equal certainty. Approximately 90% of TGFs are not associated with +EIPs but are instead associated with less energetic discharge signatures (*Lu et al.*, 2011; *Cummer et al.*, 2014), such as the recently identified “slow

pulse" TGFs (*Cummer et al.*, 2011; *Pu et al.*, 2019) and those TGFs associated with unclear or weak discharge processes (*Dwyer & Uman*, 2014; *Mailyan et al.*, 2018; *Lu et al.*, 2019).

We can assess the statistical meaning of this 10-for-10 result using the approach used previously by Lyu et al. (*Lyu et al.*, 2016) and compute the likelihood of a 10-for-10 result assuming that +EIPs produce TGFs with a fixed probability p. We use a binomial distribution to identify the range of probabilities that would produce a 10-for-10 observation with greater than 5% likelihood. Any p for which the 10-for-10 likelihood is below 5% is unlikely to produce this measurement and thus interpreted as inconsistent with the observation. A straightforward calculation shows that $p = 0.74$ yields a 5% probability (0.74^{10}) of generating the 10-for-10 observation. We thus conclude that the observations are consistent with the probability p of a +EIP also being a TGF ranging from 74% to 100%. The observations presented in this study thus indicate that at least most (74%) and perhaps all (100%) +EIPs are also TGFs.

This establishes an even stronger link between TGFs and the +EIP-generating process than previous work (*Lyu et al.*, 2016), which has several important consequences. Observations and measurements of +EIPs (for example, using a three-dimensional lightning mapping array or radio broadband interferometer) are also extremely likely to contain key information about the electron acceleration process in TGFs, even in the absence of direct gamma-ray measurements. Detailed measurements of +EIPs alone, such as that recently reported by Tilles et al. (*Tilles et al.*, 2020), should thus provide valuable insight into both TGFs and highly energetic lightning leaders.

This +EIP-TGF link also enables the detection of TGFs that are not statistically discernable in satellite gamma-ray measurements alone. The two new TGF detections shown here are both relatively weak TGFs that failed key statistical tests for the gamma-

316 ray measurements alone. But the additional precise timing information provided by the
317 simultaneous +EIPs pointed to very short, sub-millisecond time windows to search for
318 gamma-ray pulses, and indeed in these windows, TGFs were found.

319 Lastly, the identification of two new TGFs from ground-based +EIP radio detection
320 not only illustrates the tight connection between +EIPs and TGFs, but also further
321 demonstrated the practicability of detecting a subset of TGFs from ground radio
322 measurements alone. Ground-based detection of TGFs from long-distance radio
323 measurements can strongly complement space-based detection of TGFs.

324

325 **6. Discussion and Conclusions**

326 Energetic in-cloud pulses, or EIPs, are a recently identified class of high peak-
327 current lightning events that occur sometimes during the progression of lightning in-
328 cloud negative leaders (*Lyu et al.*, 2015; *Lyu & Cummer*, 2018). They can be robustly
329 detected and reliably identified using signals from distant ground-based radio sensors.
330 In this study, an expanded radio-only search for positive polarity energetic in-cloud
331 pulses (+EIPs) yielded 10 events that occurred within the TGF-detection range of the
332 Fermi and RHESSI spacecrafts at times when gamma-ray photon data exist. The
333 simultaneous gamma-ray photon data show that all 10 +EIPs are also TGFs, including
334 two TGFs not previously identified by the routine TGF identification criteria of two
335 different space-based detectors. The 10 out of 10 EIP-TGF pairs are consistent with a
336 range of 74% to 100% for the probability that a given +EIP is also a TGF. Remarkably,
337 the identification of two previously unreported new TGFs from the detection of +EIPs
338 further validated their close relationship.

Collectively, the results shown in this study presented strong evidence that most and perhaps all +EIPs are TGFs. We emphasize that the converse is not true because only about 10% of all TGFs are associated with high peak current +EIPs. The definitive EIP-TGF connection also implies a link between the processes involved in TGF production and the processes that produce strong, transient, >100 kA equivalent peak current pulses during the propagation of upward negative leaders. A recent study on EIPs using very high frequency (VHF) broadband interferometry and electromagnetic field measurements (*Tilles et al.,* 2020) conducted a detailed analysis on the radio emission of the +EIP source. Those results, plus our new findings here, continue to suggest that the +EIP sferic is, to a large extent, not produced by normal lightning leader processes. This is similar to what has been found previously for a distinct class of TGFs, the so-called "isolated slow pulse" TGFs (*Cummer et al.,* 2011; *Pu et al.,* 2019). The +EIP and the "slow pulse" processes do share several common features between them, including the close temporal association with TGFs, the occurrence the pulse during upward negative initial leaders, and the time scale of the pulse (~50-100 μs). However, the peak radiated field of +EIPs is typically more than an order of larger than that of the slow pulses, and the waveform of a typical +EIP is much more complex than a slow pulse. Both +EIPs and the slow pulses appear to be produced at least partly by the relativistic electron acceleration in the TGF production (*Dwyer,* 2012; *Liu & Dwyer*, 2013) and not by standard lightning processes.

An important element of this research is the identification of two previously unreported new TGFs from the detection of +EIPs. This finding not only adds key support to the EIP-TGF connection, but also, for the first time, experimentally demonstrates the idea of detecting a subset of TGFs from ground-based radio measurements alone (*Lyu et al.,* 2016). The ability to detect a subset of TGFs through

ground-based, radio-only measurements will significantly improve obtaining more detailed measurements of the lightning processes responsible for producing TGFs. This type of TGF detection can be a valuable addition to satellite gamma-ray detector-based detection, especially during time windows or in locations where space-based detectors are not available.

These results also strengthen the connection between TGFs and transient luminous events, specifically in the form of elves (*Lyu et al.,* 2015), seen as optical emissions at the altitude of lower ionosphere because of the transient field change from energetic electromagnetic field pulses. Modeling suggested that elves may accompany with TGFs associated with EIPs (*Liu et al.,* 2017). This connection was confirmed by a recent study reporting a simultaneous observation of a TGF and elve (*Neubert et al.,* 2020) associated with a radio pulse that seems likely to also have been a +EIP. The detection of +EIPs from the ground is thus a useful method to perform observations and detailed studies of the connection between different energetic atmospheric electricity processes including EIPs, TGFs, and elves during thunderstorms.

Acknowledgment

The authors would like to acknowledge support from the National Science Foundation Dynamic and Physical Meteorology program (grant AGS-2026304), the Open Grants of the State Key Laboratory of Severe Weather of China (grant 2020LASW-A02), the National Science Foundation (grant ATM-0846609 and grant ATM-1935989), and the National Aeronautics and Space Administration (grant NNM11AA01A). This work complies with the AGU data policy. The radio waveforms, NLDN reported information, the RHESSI and Fermi-GBM photon counts are available

388 at XX (the link will be provided later). The Fermi BGO photon counts are also available
389 at https://heasarc.gsfc.nasa.gov/FTP/ fermi/data/gbm/daily/.

390

391 **Reference**

392 Briggs, M. S., Fishman, G. J., Connaughton, V., Bhat, P. N., Paciesas, W. S., Preece,
393 R. D., Wilson-Hodge, C., Chaplin, V. L., Kippen, R. M., von Kienlin, A., et al.
394 (2010). First results on terrestrial gamma ray flashes from the Fermi Gamma-
395 ray Burst Monitor. *Journal of Geophysical Research: Space Physics*, *115*(A7),
396 doi:10.1029/2009JA015242.
397 Briggs, M. S., Xiong, S. L., Connaughton, V., Tierney, D., Fitzpatrick, G., Foley, S.,
398 Grove, J. E., Chekhtman, A., Gibby, M., Fishman, G. J., et al. (2013). Terrestrial
399 gamma-ray flashes in the Fermi era: Improved observations and analysis
400 methods. *Journal of Geophysical Research-Space Physics*, *118*(6), 3805-3830,
401 doi:10.1002/jgra.50205.
402 Celestin, S., & Pasko, V. P. (2012). Compton scattering effects on the duration of
403 terrestrial gamma-ray flashes. *Geophysical Research Letters*, *39*,
404 doi:10.1029/2011GL050342.
405 Connaughton, V., Briggs, M. S., Holzworth, R. H., Hutchins, M. L., Fishman, G. J.,
406 Wilson-Hodge, C. A., Chaplin, V. L., Bhat, P. N., Greiner, J., von Kienlin, A.,
407 et al. (2010). Associations between Fermi Gamma-ray Burst Monitor terrestrial
408 gamma ray flashes and sferics from the World Wide Lightning Location
409 Network. *Journal of Geophysical Research-Space Physics*, *115*,
410 doi:10.1029/2010JA015681.
411 Cummer, S. A., Lu, G. P., Briggs, M. S., Connaughton, V., Xiong, S. L., Fishman, G.
412 J., & Dwyer, J. R. (2011). The lightning-TGF relationship on microsecond
413 timescales. *Geophysical Research Letters*, *38*, doi:10.1029/2011GL048099.
414 Cummer, S. A., Briggs, M. S., Dwyer, J. R., Xiong, S. L., Connaughton, V., Fishman,
415 G. J., Lu, G. P., Lyu, F. C., & Solanki, R. (2014). The source altitude, electric
416 current, and intrinsic brightness of terrestrial gamma ray flashes. *Geophysical*
417 *Research Letters, 41*(23), 8586-8593
418 Dwyer, J. R. (2012). The relativistic feedback discharge model of terrestrial gamma ray

flashes. *JOURNAL OF GEOPHYSICAL RESEARCH, 117*(A2), doi:10.1029/2011JA017160.

Dwyer, J. R., Smith, D. M., & Cummer, S. A. (2012). High-Energy Atmospheric Physics: Terrestrial Gamma-Ray Flashes and Related Phenomena. *Space Science Reviews, 173*(1), 133-196, doi:10.1007/s11214-012-9894-0.

Dwyer, J. R., & Cummer, S. A. (2013). Radio emissions from terrestrial gamma-ray flashes. *Journal of Geophysical Research-Space Physics, 118*(6), 3769-3790, doi:10.1002/jgra.50188.

Dwyer, J. R., & Uman, M. A. (2014). The physics of lightning. *Physics Reports-Review Section of Physics Letters, 534*(4), 147-241, doi:10.1016/j.physrep.2013.09.004.

Dwyer, J. R., Liu, N. Y., Grove, J. E., Rassoul, H., & Smith, D. M. (2017). Characterizing the source properties of terrestrial gamma ray flashes. *Journal of Geophysical Research-Space Physics, 122*(8), 8915-8932, doi:10.1002/2017JA024141.

Fishman, G. J., Bhat, P. N., Mallozzi, R., Horack, J. M., Koshut, T., Kouveliotou, C., Pendleton, G. N., Meegan, C. A., Wilson, R. B., Paciesas, W. S., et al. (1994). Discovery of intense gamma-ray flashes of atmospheric origin. *Science, 264*(5163), 1313-1316, doi:10.1126/science.264.5163.1313.

Liu, N., & Dwyer, J. R. (2013). Modeling terrestrial gamma ray flashes produced by relativistic feedback discharges. *Journal of Geophysical Research-Space Physics, 118*(5), 2359-2376, doi:10.1002/jgra.50232.

Liu, N., Dwyer, J. R., & Cummer, S. A. (2017). Elves Accompanying Terrestrial Gamma Ray Flashes. *Journal of Geophysical Research-Space Physics, 122*(10), 10563-10576, doi:10.1002/2017JA024344.

Lu, G., Blakeslee, R. J., Li, J., Smith, D. M., Shao, X.-M., McCaul, E. W., Buechler, D. E., Christian, H. J., Hall, J. M., & Cummer, S. A. (2010). Lightning mapping observation of a terrestrial gamma-ray flash. *Geophysical Research Letters, 37*(11), doi:10.1029/2010GL043494.

Lu, G., Cummer, S. A., Li, J. B., Han, F., Smith, D. M., & Grefenstette, B. W. (2011). Characteristics of broadband lightning emissions associated with terrestrial gamma ray flashes. *Journal of Geophysical Research-Space Physics, 116*, doi:10.1029/2010JA016141.

Lu, G., Zhang, H. B., Cummer, S. A., Wang, Y. P., Lyu, F. C., Briggs, M., Xiong, S.

L., & Chen, A. (2019). A comparative study on the lightning sferics associated with terrestrial gamma-ray flashes observed in Americas and Asia. *Journal of Atmospheric and Solar-Terrestrial Physics, 183*, 67-75, doi:10.1016/j.jastp.2019.01.001.

Lyu, F., Cummer, S. A., & McTague, L. (2015). Insights into high peak current in-cloud lightning events during thunderstorms. *Geophysical Research Letters, 42*(16), 6836-6843, doi:10.1002/2015GL065047.

Lyu, F., Cummer, S. A., Briggs, M., Marisaldi, M., Blakeslee, R. J., Bruning, E., Wilson, J. G., Rison, W., Krehbiel, P., Lu, G., et al. (2016). Ground detection of terrestrial gamma ray flashes from distant radio signals. *Geophysical Research Letters, 43*(16), 8728-8734, doi:10.1002/2016GL070154.

Lyu, F., & Cummer, S. A. (2018). Energetic Radio Emissions and Possible Terrestrial Gamma-Ray Flashes Associated With Downward Propagating Negative Leaders. *Geophysical Research Letters, 45*(19), 10764-10771, doi:10.1029/2018GL079424.

Lyu, F., Cummer, S. A., Krehbiel, P. R., Rison, W., Briggs, M. S., Crame, E., Roberts, O., & Stanbro, M. (2018). Very High Frequency Radio Emissions Associated With the Production of Terrestrial Gamma-Ray Flashes. *Geophysical Research Letters, 45*(4), 2097-2105, doi:10.1002/2018GL077102.

Mailyan, B. G., Nag, A., Murphy, M. J., Briggs, M. S., Dwyer, J. R., Rison, W., Krehbiel, P. R., Boggs, L., Bozarth, A., Cramer, E. S., et al. (2018). Characteristics of Radio Emissions Associated With Terrestrial Gamma-Ray Flashes. *Journal of Geophysical Research-Space Physics, 123*(7), 5933-5948, doi:10.1029/2018JA025450.

Marisaldi, M., Fuschino, F., Labanti, C., Galli, M., Longo, F., Del Monte, E., Barbiellini, G., Tavani, M., Giuliani, A., Moretti, E., et al. (2010). Detection of terrestrial gamma ray flashes up to 40 MeV by the AGILE satellite. *Journal of Geophysical Research: Atmospheres, 115*(A3), doi:10.1029/2009JA014502.

Neubert, T., Ostgaard, N., Reglero, V., Blanc, E., Chanrion, O., Oxborrow, C. A., Orr, A., Tacconi, M., Hartnack, O., & Bhanderi, D. D. V. (2019). The ASIM Mission on the International Space Station. *Space Science Reviews, 215*(2), doi:10.1007/s11214-019-0592-z.

Neubert, T., Ostgaard, N., Reglero, V., Chanrion, O., Heumesser, M., Dimitriadou, K.,

Christiansen, F., Budtz-Jorgensen, C., Kuvvetli, I., Rasmussen, I. L., et al. (2020). A terrestrial gamma-ray flash and ionospheric ultraviolet emissions powered by lightning. *Science, 367*(6474), 183-186, doi:10.1126/science.aax3872.

Østgaard, N., Gjesteland, T., Stadsnes, J., Connell, P. H., & Carlson, B. (2008). Production altitude and time delays of the terrestrial gamma flashes: Revisiting the Burst and Transient Source Experiment spectra. *Journal of Geophysical Research-Atmospheres, 113*(A2), doi:10.1029/2007ja012618.

Østgaard, N., Gjesteland, T., Carlson, B. E., Collier, A. B., Cummer, S. A., Lu, G., & Christian, H. J. (2013). Simultaneous observations of optical lightning and terrestrial gamma ray flash from space. *Geophysical Research Letters, 40*(10), 2423-2426, doi:10.1002/grl.50466.

Pu, Y., Cummer, S. A., Lyu, F., Briggs, M., Mailyan, B., Stanbro, M., & Roberts, O. (2019). Low Frequency Radio Pulses Produced by Terrestrial Gamma-Ray Flashes. *Geophysical Research Letters, 46*(12), 6990-6997, doi:10.1029/2019GL082743.

Roberts, O. J., Fitzpatrick, G., Stanbro, M., McBreen, S., Briggs, M. S., Holzworth, R. H., Grove, J. E., Chekhtman, A., Cramer, E. S., & Mailyan, B. G. (2018). The First Fermi-GBM Terrestrial Gamma Ray Flash Catalog. *Journal of Geophysical Research-Space Physics, 123*(5), 4381-4401, doi:10.1029/2017JA024837.

Shao, X. M., Hamlin, T., & Smith, D. M. (2010). A closer examination of terrestrial gamma-ray flash-related lightning processes. *Journal of Geophysical Research-Space Physics, 115*(A00E30), doi:10.1029/2009JA014835.

Smith, D. M., L. I. Lopez, R. P. Lin, & Barrington-Leigh, C. P. (2005). Terrestrial gamma-ray flashes observed up to 20 MeV. *Science, 307*(5712), 1085-1088, doi:10.1126/science.1107466.

Stanley, M. A., Shao, X. M., Smith, D. M., Lopez, L. I., Pongratz, M. B., Harlin, J. D., Stock, M., & Regan, A. (2006). A link between terrestrial gamma-ray flashes and intracloud lightning discharges. *Geophysical Research Letters, 33*(6), doi:10.1029/2005GL025537.

Tilles, J. N., Krehbiel, P. R., Stanley, M. A., Rison, W., Liu, N., Lyu, F., Cummer, S. A., Dwyer, J. R., Senay, S., Edens, H., et al. (2020). Radio Interferometer

518 Observations of an Energetic in-Cloud Pulse Reveal Large Currents Generated
519 by Relativistic Discharges. *Journal of Geophysical Research-Atmospheres*,
520 *125*(20), e2020JD032603, doi:10.1029/2020jd032603.
521 Xu, W., Celestin, S., Pasko, V. P., & Marshall, R. A. (2019). Compton Scattering
522 Effects on the Spectral and Temporal Properties of Terrestrial Gamma-Ray
523 Flashes. *Journal of Geophysical Research-Space Physics*, *124*(8), 7220-7230,
524 doi:10. 1029/2019JA026941.
525 Zhang, H., Lu, G., Lyu, F., Ahmad, M. R., Qie, X., Cummer, S. A., Xiong, S., & Briggs,
526 M. S. (2020). First Measurements of Low-Frequency Sferics Associated With
527 Terrestrial Gamma-Ray Flashes Produced by Equatorial Thunderstorms.
528 *Geophysical Research Letters*, *47*(17), e2020GL089005,
529 doi:10.1029/2020gl089005.

530